

New high-entropy alloy superconductor

Naoki Ishizu¹

¹ *Department of Electrical Engineering, Faculty of Engineering, Fukuoka Institute of Technology, 3-30-1 Wajiro-higashi, Higashi-ku, Fukuoka 811-0295, Japan*

Jiro Kitagawa¹

¹ *Department of Electrical Engineering, Faculty of Engineering, Fukuoka Institute of Technology, 3-30-1 Wajiro-higashi, Higashi-ku, Fukuoka 811-0295, Japan*

Abstract

High-entropy alloys are a new class of alloys, and attract much attention due to their unique properties. Since the discovery of a superconducting high-entropy alloy (HEA) in 2014, the materials research on HEA superconductor is a hot topic. We have found that $\text{Hf}_{21}\text{Nb}_{25}\text{Ti}_{15}\text{V}_{15}\text{Zr}_{24}$ body-centered-cubic (BCC) HEA is a new superconductor with the superconducting critical temperature T_c of 5.3 K. We briefly discussed the comparison of cocktail effect of T_c among BCC HEA superconductors.

Keywords: high-entropy alloy, superconductor, cocktail effect

Email address: j-kitagawa@fit.ac.jp (Jiro Kitagawa¹)

1. Introduction

There are two well accepted definitions[1] for high-entropy alloys: alloys containing at least five elements with the atomic percentage of i -th element X_i $5\% \leq X_i \leq 35\%$, and alloys with the mixing entropy S_{mix} larger than $1.5R$, where R is the gas constant. S_{mix} for a n elements alloy is given by $-R \sum_{i=1}^n x_i \ln x_i$, where x_i is the mole fraction of i -th component.

A high-entropy alloy (HEA) generally forms a simple crystalline structure like face-centered-cubic, body-centered-cubic (BCC) or close-packed hexagonal. Focusing on the superconducting HEAs, BCC materials are well studied, however, there are only several reports[2, 3, 4]. This fact motivated us to carry out the materials research on HEA superconductors. Recently equimolar BCC HfNbTiVZr is reported[5], however, a secondary phase appears during annealing. We have searched a BCC Hf-Nb-Ti-V-Zr HEA, which is stable even after annealing, by changing the atomic composition, and checked the possible superconductivity. In this article, we report a thus found HEA superconductor $\text{Hf}_{21}\text{Nb}_{25}\text{Ti}_{15}\text{V}_{15}\text{Zr}_{24}$.

2. Materials and methods

The polycrystalline sample $\text{Hf}_{21}\text{Nb}_{25}\text{Ti}_{15}\text{V}_{15}\text{Zr}_{24}$ was made by a home-made arc furnace. The constituent elements of Hf (99.9%), Nb (99.9%), Ti (99.5%), V (99.9%) and Zr (99%) with the stoichiometric composition were placed on a water-cooled Cu hearth and arc-melted in an Ar atmosphere. The annealing condition was 800 °C for 4 days in an evacuated quartz tube. The measurement methods of sample characterization and temperature dependences of ac magnetic susceptibility χ_{ac} (T) and electrical resistivity ρ (T) are described in the previous papers of our team[6, 7].

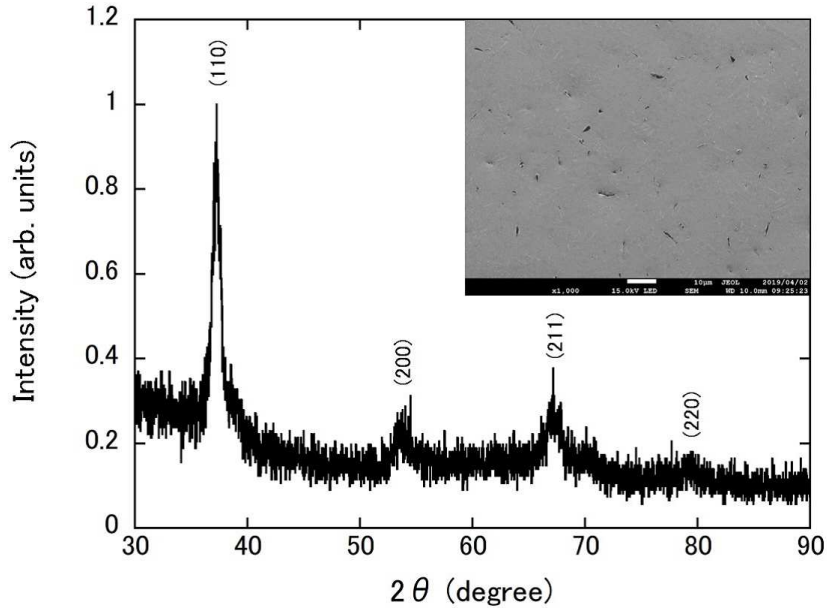


Figure 1: X-ray diffraction pattern of $\text{Hf}_{21}\text{Nb}_{25}\text{Ti}_{15}\text{V}_{15}\text{Zr}_{24}$. The inset is the back-scattered electron (15 keV) image of the sample.

3. Results and discussion

Figure 1 shows the X-ray diffraction pattern of $\text{Hf}_{21}\text{Nb}_{25}\text{Ti}_{15}\text{V}_{15}\text{Zr}_{24}$. The diffraction peaks can be well indexed by a BCC structure with the lattice parameter $a=3.401$ Å. Back-scattered electron image obtained by a field emission scanning electron microscope with electron beams of 15 keV is shown in the inset of Fig. 1. Although there are voids with small black areas, no obvious impurity phases are detected. The atomic composition obtained by an energy dispersive X-ray measurement is $\text{Hf}_{21.2(3)}\text{Nb}_{25.3(3)}\text{Ti}_{13.8(2)}\text{V}_{15.4(5)}\text{Zr}_{24.3(1)}$, which is in agreement with the starting composition.

Shown in Fig. 2 is χ_{ac} (T) of $\text{Hf}_{21}\text{Nb}_{25}\text{Ti}_{15}\text{V}_{15}\text{Zr}_{24}$. The real part of χ_{ac} , χ'_{ac} , exhibits the diamagnetic signal below the superconducting critical temperature $T_c=5.3$ K, which is determined as being the intercept of the

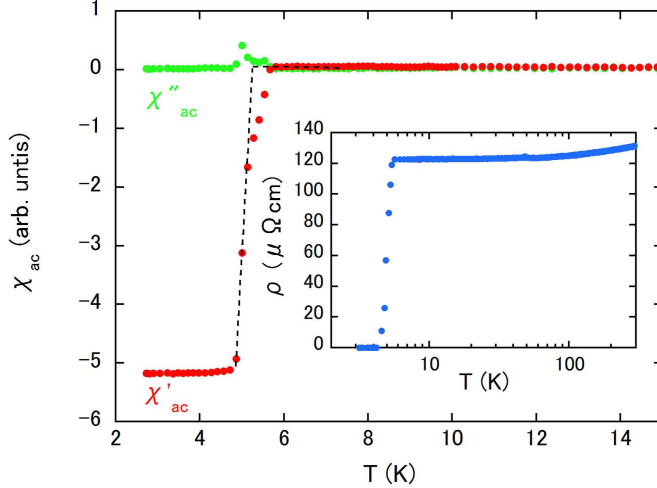


Figure 2: Temperature dependences of χ_{ac} and ρ of $\text{Hf}_{21}\text{Nb}_{25}\text{Ti}_{15}\text{V}_{15}\text{Zr}_{24}$.

linearly extrapolated diamagnetic slope with the normal state signal[3, 7] (see the broken lines in Fig. 2). The imaginary χ_{ac} , χ''_{ac} , shows a peak, which is also characteristic of superconductors. In the inset of Fig. 2, ρ (T) exhibits a very weak temperature dependence, reflecting the atomic disorder. ρ rapidly drops below approximately T_c and shows the zero resistivity.

One of the interesting properties of HEAs is the cocktail effect, which means an enhancement of physical property beyond the simple mixture of those of constituent elements. Table 1 shows the comparison of cocktail effect of T_c , S_{mix}/R and valence electron concentration (VEC) per atom of BCC HEA superconductors. We also list a reference material $\text{Nb}_{66}\text{Ti}_{33}$, that does not fulfill both of two HEA-definitions mentioned above. Following the method reported in ref.[2], the cocktail effect of T_c is evaluated by $T_c^{\text{obs.}}/T_c^{\text{base}}$, where $T_c^{\text{obs.}}$ and T_c^{base} are the experimental T_c and T_c obtained by averaging

Table 1: Comparison of cocktail effect of T_c , S_{mix}/R and valence electron concentration (VEC) per atom among BCC HEA superconductors. $T_c^{\text{obs.}}$ and T_c^{base} are the experimental T_c and T_c obtained by averaging T_c 's of the constituent elements weighted by each atomic percentage, respectively.

Compound	$T_c^{\text{obs.}}$ (K)	T_c^{base} (K)	$T_c^{\text{obs.}}/T_c^{\text{base}}$	S_{mix}/R	VEC	ref.
Hf ₂₁ Nb ₂₅ Ti ₁₅ V ₁₅ Zr ₂₄	5.3	3.30	1.61	1.586	4.4	this work
Ta ₃₄ Nb ₃₃ Hf ₈ Zr ₁₄ Ti ₁₁	7.3	4.72	1.55	1.453	4.67	[2]
Nb ₂₀ Re ₂₀ Hf ₂₀ Zr ₂₀ Ti ₂₀	5.3	2.42	2.2	1.609	4.8	[4]
(TaNb) _{0.7} (ZrHfTi) _{0.3}	8.0	4.93	1.62	1.195	4.7	[3]
(TaNb) _{0.6} (ZrHfTi) _{0.4}	7.56	4.28	1.77	1.528	4.6	[3]
(TaNb) _{0.5} (ZrHfTi) _{0.5}	6.46	3.63	1.78	1.589	4.5	[3]
(TaNb) _{0.16} (ZrHfTi) _{0.84}	4.52	1.41	3.21	1.473	4.16	[3]
Nb ₆₆ Ti ₃₃	9.2	6.34	1.45	0.6365	4.55	[3]

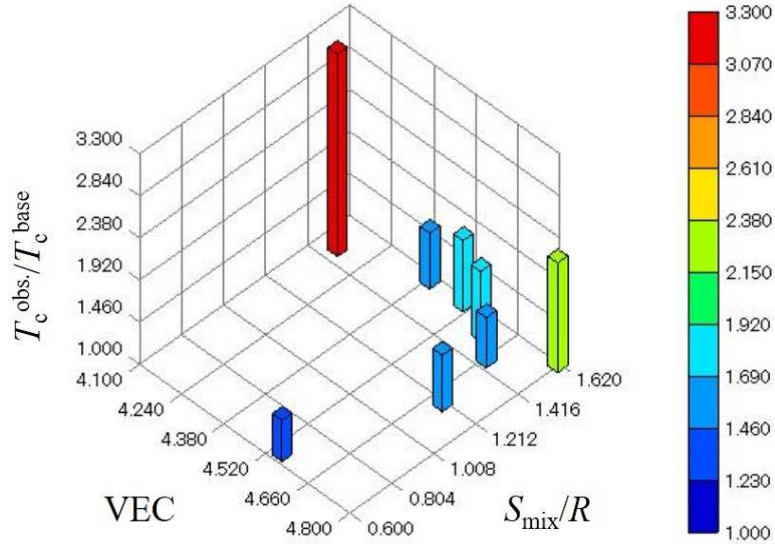


Figure 3: 3D bar graph of $T_c^{\text{obs.}}/T_c^{\text{base}}$ as a function of S_{mix}/R and VEC.

T_c 's of the constituent elements weighted by each atomic percentage, respectively. T_c^{base} plays a role of base line in order to know an enhancement of T_c due to a mixing of constituent elements, and a larger $T_c^{\text{obs.}}/T_c^{\text{base}}$ indicates a strong cocktail effect. VEC is an important factor deciding T_c , that is well known as the Matthias rule[8], in which the VEC dependence of T_c for crystalline d -electron systems shows a maximum at approximately VEC=4.5 and T_c steeply decreases to zero around VEC=4.0 or 5.3. However, the BCC HEA superconductors[3] preserve a rather high T_c compared to the prediction value of the Matthias rule especially at the side of VEC smaller than 4.5. Keeping this in mind, we made a three-dimensional bar graph in Fig. 3 by using the numerical values listed in Table 1. The enhancement of T_c in each HEA is stronger than that of $\text{Nb}_{66}\text{Ti}_{33}$. The value of $T_c^{\text{obs.}}/T_c^{\text{base}}$ seems to increase with increasing S_{mix} . We note here that $(\text{TaNb})_{0.16}(\text{ZrHfTi})_{0.84}$ shows the strong T_c enhancement, although S_{mix}/R of this compound is relatively small. VEC of $(\text{TaNb})_{0.16}(\text{ZrHfTi})_{0.84}$ is 4.16, where T_c is suppressed to nearly zero in the VEC dependence of T_c by the Matthias rule. This result suggests that the VEC also somewhat affects the enhancement of T_c in HEA superconductors.

4. Summary

We have found that $\text{Hf}_{21}\text{Nb}_{25}\text{Ti}_{15}\text{V}_{15}\text{Zr}_{24}$ is a new member of HEA superconductors. It crystallizes into the BCC structure with $a=3.401 \text{ \AA}$, and T_c is 5.3 K. The cocktail effect of T_c in BCC HEA superconductors might be affected by S_{mix} and/or VEC.

Acknowledgments

J.K. is grateful for the support provided by Comprehensive Research Organization of Fukuoka Institute of Technology.

References

- [1] M. C. Gao, J. -W. Yeh, P. K. Liaw, and Y. Zhang, *High-Entropy Alloys: Fundamentals and Applications*, (Cham: Springer, 2015), p. 10.
- [2] P. Koželj, S. Vrtnik, A. Jelen, S. Jazbec, Z. Jagličić, S. Maiti, M. Feuerbacher, W. Steurer, and J. Dolinšek, *Phys. Rev. Lett.* **113** (2014) 107001.
- [3] F. von Rohr, M. J. Winiarski, J. Tao, T. Klimczuk, and R. J. Cava, *Proc. Natl. Acad. Sci. U. S. A.* **113** (2016) E7144.
- [4] S. Marik, M. Varghese, K. P. Sajilesh, D. Singh, and R. P. Singh, *J. Alloys and Compd.* **769** (2018) 1059.
- [5] V. Pacheco, G. Lindwall, D. Karlsson, J. Cedervall, S. Fritze, G. Ek, P. Berastegui, M. Sahlberg, and Ulf Jansson, *Inorg. Chem.* **58** (2019) 811.
- [6] J. Kitagawa and K. Sakaguchi, *J. Magn. Magn. Mater.* **468** (2018) 115.
- [7] S. Hamamoto and J. Kitagawa, *Mater. Res. Express* **5** (2018) 106001.
- [8] B. T. Matthias, *Phys. Rev.* **97** (1955) 74.